UNIVERSITY OF CALIFORNIA, IRVINE

Joining Blood and Ferric Chloride in a Microfluidic Device

THESIS

Submitted for the degree of

MASTER OF SCIENCE

In Biomedical Engineering

By

Krystopher Lawrence

Thesis Committee:
Abraham Lee, Chair
Michelle Digman
Wendy Liu

Contents

Chapter 1

1.1 Problem Statement

Venous thromboembolism is when pathological blood clotting occurs within the veins. These can most commonly occur in the legs, though deep veins elsewhere in the body, particularly the arms and brain, can be sites of embolism formation (1). Deep vein thrombosis in the legs can present symptoms such as swelling, redness, tenderness (1), and pain (2). When the embolism ends up in the lungs, it is called pulmonary embolism, and may cause symptoms such as difficulty breathing, chest pain, dizziness, rapid heartbeat, hyperventilation, and even coughing up blood (1). Pulmonary embolism following a stroke is possible, but according to literature is not commonly observed (2). However, patients who experienced acute stroke can still die of sudden death due to pulmonary embolism (2). Patients with less mobility, such as limb paralysis, are more likely to experience venous thromboembolism following stroke versus patients with higher mobility (3). A proportion, about one in six, of all strokes are cardioembolic, meaning that the thrombus forms in the heart, such as in the myocardium, the left ventricle, or the mitral valve (4). As of the 1980d, a lack of validated diagnostic criteria and co-occurrence of atherosclerosis in the brain made it difficult to confirm a case of

cardioembolism.

Venous thromboembolism, once discovered by imaging, is treated with anticoagulants. Heparin, whether in the low-molecular weight or unfractionated form, is a common choice (1). The former can be dosed based on weight without having to monitor activated partial thromboelastin time results, a routine coagulation screening test (1). However, unfractionated heparin is reversible with protamine and has a shorter half-life, making it more ideal for patients also receiving thrombolysis treatment (1). Patients without full renal function can also benefit from unfractionated heparin because clearance of the low-molecular-weight heparin may be inefficient and lead to accumulation in the body (1). If complications with heparin occur, there are non-oral alternatives which include fondaparinux, argatroban, and lepirudin (1). There are three stages of treatment: an acute stage in the days and up to a couple weeks following the embolism, a maintenance period of a few months during which the patient should also rest, and a longer term extended period of treatment (1).

A 2005 study on cardiovascular events following acute pulmonary embolism separated the patients into two groups: those who experienced an idiopathic venous thromboembolism and those who had transient risk factors, which would be if the embolism occurred following trauma, surgery, pregnancy, the use of oral contraceptives, or more than a week of immobilization (5). Patients with a first episode of pulmonary embolism had higher rates of arterial and venous incidents within 3 years, and these cardiovascular events were also the most common cause of death for these patients (5). Idiopathic pulmonary embolism showed more cardiovascular events than in pulmonary embolism with transient risk factors (5). The latter group didn't even present arterial events. Most cardiovascular events occurred after treatment with anticoagulants, but prolonging oral anticoagulant use increases the risk for bleeding complications and needs to be monitored (5). The secondary venous events for idiopathic pulmonary embolism were most often another pulmonary embolism (5). In general, anticoagulants are known not to work for preventing embolism in all patients, and between 5 and 45% of patients still experience cardiovascular events after treatment (6).

Deep vein thrombosis and pulmonary embolism are a major disease burden treated mainly by

direct oral anticoagulants (1). There are 10 million cases of venous thromboembolism around the world per year, and the economic burden of this disease in the United States alone is estimated to be up to $10 billion (22). As imaging and detection methods improve, alongside an aging population and increase in comorbid conditions such as obesity, heart failure and cancer, incident rate is also increasing (1). The morbidity rate is high, with 20% of patients with pulmonary embolism who die before or within 30 days of diagnosis, and 30% of patients have a recurring instance within 10 years (1).

1.2 Proposed solution

Microfluidics can provide inexpensive and easily reproducible platforms for experiments involving hematologic and microvascular processes (7). The main advantage to microfluidics is the tight control of a dynamic fluidic environment on the microscale (7). Whereas parallel flow chambers, the previous technology, would need liters of blood to run a high shear experiment, an experiment of that time and length scale only needs microliters per minute for high shear in a microfluidic device (20). The 2014 study with Li et al could control a range of initial shear rates from 500 to 10,000 s^{-1} to demonstrate that thrombi formed at higher shear rates were more likely to detach and therefore embolize (6). These are helpful ranges because venous shear rates are around 100 to 200 s^{-1}, arterial shear rates are 1,000 to 2,000 s^{-1}, and pathological shear rates can go from 10,000 up to 100,000 s^{-1} (8). Adhesion of platelets to coagulation factors, for example VWF can be dependent on shear (8).

Experimentation with microfluidic devices also allow for tight control over biochemistry and channel geometry in a clotting system for copying the conditions in diseases of interest (20). Venous blood clots are rich in fibrin, while arterial blood clots are rich in platelets (9). This was shown to be because fibrin deposition decreases with increasing shear rate (9). A microfluidic device with perpendicular cross-flows of thrombin and fibrinogen helped demonstrate how hemodynamics affect the fibrin assembly process (9). Shear rate was variable by simply varying the height of the media

above the thrombin channel relative to the fibrinogen channel (9). Flux of thrombin through the membrane separating its channel from the fibrinogen channel was then reported to change with changing shear rate (9). In the Muthard et al paper, initial shear wall stress was set by the flow rate of the upstream pump (10).

In microfluidics, it's also easy to see spatiotemporal changes in the structure and composition of clots using fluorescence microscopy since microfluidic devices are typically fabricated with transparent material (20). The small volumes of blood at this scale still have enough platelets and coagulation factors for statistically significant results (20).

The rectangular shape of typical microfluidic channels can interrupt flow patterns when trying to emulate physiological conditions, however (20). To get around this, some groups use a cylindrical material that can be removed later for PDMS to cure around, such as an optical fiber (20). The fiber could then create a stenosed region by being notched by a razor blade with sandpaper wrapped on the blade (20).

The low Reynolds number of the flow in microfluidic devices is a limitation, though. Higher Reynolds numbers are found in pathological flows of arterial stenosis, so the recirculation vortex distal of such a stenosis would be impossible in a microfluidic device under regular creeping flow (20). My lab's LCAT system could create vortices, but they would be produced by acoustic transduction instead of the flow in the device. The vortices would have to be known and controlled with acoustic frequency instead of being a studied variable.

Chapter 2 Background

The ferric chloride thrombosis model in mice consists of placing a small piece of paper that has been soaked in $FeCl_3$ aqueous solution onto the exposed carotid artery of a mouse. Kurz et al were the first to develop this model, but in rats, and had based it on an electrically induced injury model that worked only with iron-containing electrodes. The paper applied to the artery had been dipped in solutions

varying from 5 to 65% $FeCl_3$ and a temperature probe would indicate when the artery became occluded. Time to occlusion was the varying parameter measured as a result of applying different concentrations of ferric chloride. Sixty minutes was the maximum time given for the vessel to occlude, so if it didn't occlude, 60 minutes was taken as the result. Time to occlusion decreased with increased ferric chloride concentration. The 50% ferric chloride solution application was difficult to be inhibited by heparin, so the researchers selected 35% as the preferred concentration for future studies, with a time to occlusion between 20 and 25 minutes. After 10 minutes of application, the luminal surface was observed to be stripped of endothelial cells and covered with adhered platelets and a few red and white blood cells mixed in. Then by about 20 minutes, an occlusive thrombosis with platelets, fibrin, and erythrocytes would be present. (11)

Endothelial cells are found to be removed by $FeCl_3$ applied to the exterior of the vessel. It used to be thought that this damage to the vessel would initiate thrombosis. However, the inner layers of the vessel are not exposed, so only basement membrane components could have contributed to thrombus formation (14). What appears to be a denuded endothelial surface might actually be remnants of red blood cells transiently adhering to the endothelium (15). One paper observed that "ferric ion-filled spherical bodies" appear on the endothelial cells which platelets then adhere to and form aggregates (14). Another found that platelets do not adhere directly to the endothelium but mostly to erythrocytes that have firmly adhered to the endothelium (15). Platelets adhered to these red blood cells then initiate thrombosis (15). By testing in scenarios with deficiencies of von Wilebrand factor and GPIb-alpha, the paper demonstrated that neither is required for $FeCl_3$-induced erythrocyte adhesion. The VWF deficiency resulted in a slower rate of thrombus formation, but the thrombosis still occurred because platelet recruitment could still occur, but merely slowed down (15). GPIb-alpha deficiency also slows the binding between platelets and erythrocytes, as it is a receptor on the platelets (15).

Most animal models use ferric chloride or laser activity to damage the vessel with free radicals and cause thrombosis even in non-murine animal models (18). There is also intraluminal injury, by which the vessel is opened and mechanically scratched to remove the intima, exposing collagen and other

extracellular matrix components to the platelets and clotting factors to start thrombosis (18). Electrolytic injury applied to the arterial surface makes for a newer mouse model, and newer ones are being discovered but have not yet been standardized (18). Thrombosis is not just blood clotting, however, it is pathological blood clotting within a blood vessel without there being injury or bleeding that would necessitate a clot for hemostasis (18).

Thrombosis models on the veins are most useful for research relating to deep vein thrombosis, but mouse veins are fragile and have varying anatomy concerning their branches (18). Nevertheless, mouse vein-based thrombosis models have still helped confirm the effects of low flow in valve pockets, genetic risk factors that are orthologs in humans, and microvesicles (18), as well as elucidating the role of inflammatory cells in venous thrombosis (18). Zebrafish can also be studied for hemostasis and thrombus formation because they share ortholog genes with humans for coagulation, anticoagulation, and platelet signaling proteins (18). The same ferric chloride and laser activity models exist but are performed on zebrafish larvae only days after fertilization (18). The larvae are immobilized in agarose and then coated in ferric chloride or phenylhydrazine to induce thrombosis in the thin tail (18). Again, time to occlusion is the main way to measure an output parameter (18). The laser-induced model in zebrafish results in a half-moon structure that extends from the endothelium to the lumen of the vessel, with thrombocyte presence verified by antibody staining (18). Meanwhile, the ferric chloride model results in fibrin forming in clusters within the vessel (18). These animal models are limited in terms of mechanisms being poorly understood and poorly resembling actual pathological processes. The main advantage with these models is that the roles of individual components can be studied through genetic knockdowns or through functional inactivation. Multiple models are still needed in the process of testing a new antithrombotic drug for humans (18).

Blood vessels in the human body range from 1 to 3 cm in the aorta down to 3 to 10 um in the capillaries (19). Photolithography techniques for fabricating microfluidic devices can create features all the way down to 100nm (19), depending on the technique and skill of the handler. Adhesion of platelets onto denuded vessel walls is shear-dependent and highly regulated by complex flow, which can be

studied easily in microfluidics (19). Under arterial flow conditions, von Willebrand Factor (VWF) is important for thrombus formation, while fibronectin and fibrinogen are more important at the lower, venous shears (19). VWF and fibrinogen form important substrates for clot formation in various prosthetics, including left ventricular assist devices (19). VWF captures platelet receptor GPIba in a transient shear-dependent interaction best studied under flow (19). There already exist microfluidic devices for measuring bleeding risk, particularly one which can monitor multiple output parameters including immobilized platelet number and aggregate morphology (19). Flow devices have been used to evaluate von Willebrand Disease, which is a deficiency in VWF and hemostasis, with varying linear shear rates and comparing clotting at the wall under a physiological blood flow (19).

For studying thrombosis in pathological blood flows, microfluidics are easy to use with good versatility, appropriate scale, and decent control of fluid conditions (20). The transparency of the devices are ideal for observation of spatiotemporal changes in clot structure and composition under a fluorescent microscope (20). Antibodies against blood components can be used to fluorescently track thrombosis (20). High shear experiments in microfluidics need far less blood than the previous technology of parallel flow chambers: microliters per minute versus liters of blood for the same time and length scale (20).

The platform in our lab is capable of vascularized micro-organs that are perfused by physiological flow and basically contains tissue chambers with which extracellular matrix and cells are loaded (21). Cancer cell studies have traditionally been performed in 2D monoloayers, which ignore the extracellular matrix, stromal cells, and vasculature of a tumor which have normally important functions *in vivo* in 3D (21). Experiments in the field with tumor spheroids address some of those problems but they lack vasculature, and the highly invasive tumor cells don't readily form spheroids, thus the tumor spheroid is inappropriate for some cancer cell types (21). By culturing human colorectal cancer or breast cancer with stromal cells and endothelial cells, a vascular network is formed within a week, and the tumor cells form small spheroids within and around the microvessels, like a tumor *in vivo* (21). Then drugs focused on either the vasculature itself or the glycolytic metabolism of the tumor cells (21). The platform proves

itself to be simple and effective for microtumor growth and drug testing, not requiring external pumps, tubing, or robotics, and supportive of non-spheroidal tumor types (21).

Chapter 3 Methods and Experimental Design

The first mold to produce devices was fabricated with SU-8 2050 negative photoresist on a silicon wafer via photolithography. For photolithography, the silicon wafer was first rinsed by deionized water and air-dried with a nitrogen gun. Then, the remaining moisture was evaporated off in the 65C oven for a couple of minutes. The wafer was then put in the Laurell spinner for 30s on 500rpm with an acceleration of 100rpm/s and then 20s at 3250rpm to get the SU-8 2050 down to 50um thick on the wafer. The soft bake step was in 65C and then 95C. The wafer was then exposed to UV light for 16 seconds and returned to the two ovens for post-exposure bake. After development in a sonicated bath with SU-8 developer, the wafer could then be rinsed with IPA and dried with the nitrogen gun.

Then, the first devices worked on were single layer devices poured from 10:1 PDMS basement to cross-linker by mass. For example, if a mold required 20g of PDMS, 18.2g basement plus 1.8g cross-linker would be the minimum put together to equal 20g. Practically, I added 22.7g of basement with 2.3g of cross-linker in order to ensure that I have 20g of PDMS to pour out of the weighing boat. 20g of basement plus 2g of cross-linker should also work.

Uncured PDMS was then degassed in a vacuum chamber until air bubbles were minimal. This could take 20 to 40 minutes depending on the amount of PDMS degassed at a time. The PDMS was then poured onto a mold etched onto a 3-inch silicone wafer in an 8cm diameter polystyrene dish. The wafer has (50um tall in negative photoresist SU-8) the following design microfabricated to it by photolithography.

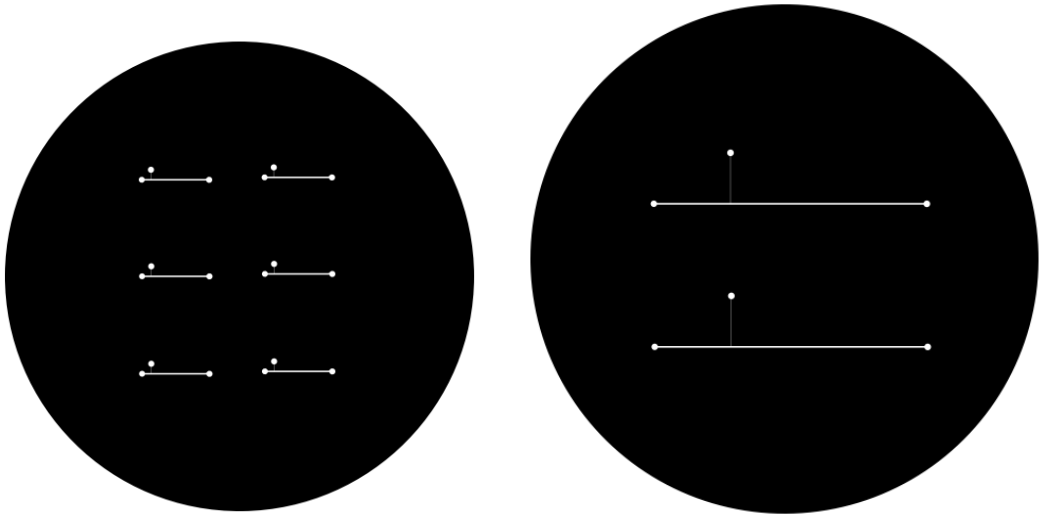

Figure 1**:** *the first two designs; the left was intended to be used with a syringe pump, whereas the right has the space for the 1cm diameter vials that supply height for hydrostatic pressure*

The main channel, for flow of whole blood was 250um in width, while the side channel was 50um wide to be able to add $FeCl_3$ solution to the system at 5, 50, and 500mM concentrations. The PDMS cured at room temperature on a level surface overnight (18h). In the morning, the mold would be transferred to a 65C oven for approximately an hour to finish curing. Following removal from the mold using a scalpel, the devices were cut to about 40 by 18mm to fit onto the 75mm by 25mm glass slides they would be bonded to. The outlet and inlet pores were punched with a 1mm hole punch.

For plasma bonding, the device layer was bonded to a 1mm sheet of manufactured PDMS, cut to a rectangular shape (40 by 20mm) that would accommodate for the size of the microfluidic design. Then the device was plasma bonded to a glass slide as a stable substrate. Plastic Nalgene vials with the bottoms cut off were "glued" to the inputs of the device using PDMS. Pipet tips inserted within the punched holes to prevent uncured PDMS from filling the channel.

The correct heights of blood and $FeCl_3$ solution were used to drive hydrostatic pressure and therefore flow in the devices. The two inputs had volumes of 500uL on top of them for high pressure, and 107uL were put on the output for low pressure. The main channel was expected to have a flow of

nearly 4 uL/s with a pressure drop of about 52 Pa. Ferric chloride dissolved in HBSS at concentrations of 5, 50, and 500mM using the same volume of 500uL over the input hole, however the narrower diameter of the FeCl3 side channel would mean that resistance would be greater and that flow in the side channel would be lower compared to the main channel. Downstream, the channel was observed under the microscope for evidence of clotting until the channel potentially clotted completely. Time to first aggregation and to occlusion in seconds after introduction of ferric chloride were measured.

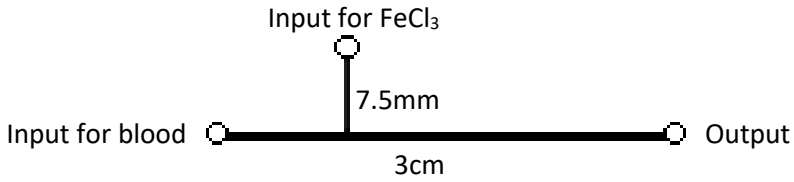

Chapter 4 Results

At first, the channel was primed with 8uL of $CaCl_2$ with the intent to get a final concentration of 0.05 M in the half a millimeter of blood that would theoretically flow down the channel. However, after four runs, the blood never travels more than about 8mm in 72 hours while the entire channel is about 3cm long, with 1.5 cm until the T-junction where the blood ought to meet the ferric chloride. However, the ferric chloride solution at 500mM did not flow either in the time given for the fluid to flow. Calcium chloride is intended to recalcify sodium citrated blood so that it could clot again, as done in the paper by Ciciliano et al (16). However, the blood available to my lab was EDTA-treated.

For the second run, the channel was primed with blood to see if that would help to get the flow starting, but then it was impossible to tell if anything changed after 72 hours. No clotting was observed, so the “blood priming” was not repeated for the third and fourth runs, performed simultaneously in a single device. After 12 hours, these third and fourth runs did not move much into the channel. The blood may have begun congealing anyway, based on a texture check with a pipet tip.

The blood no longer flowed within the vial as a fluid but moved around in soft and moist chunks when disturbed. With runs 2 through 4, the device was kept in a 37C incubator, whereas the first run was performed at room temperature. Run 4 was not primed with the calcium chloride, but the 8uL of $CaCl_2$ was placed and mixed into the input vial with 500uL of blood.

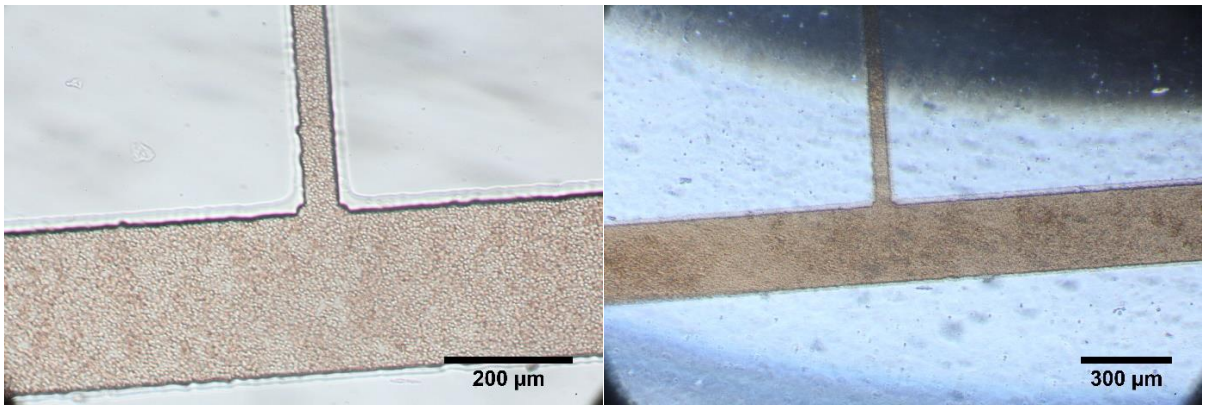

Figure 2: *Blood filling the channel in Run 2 before and after 72 hours. The channel was primed with blood and some sort of agglomeration happened but is unclear to be clotting or when it occurred. Flow is expected to have been negligible.*

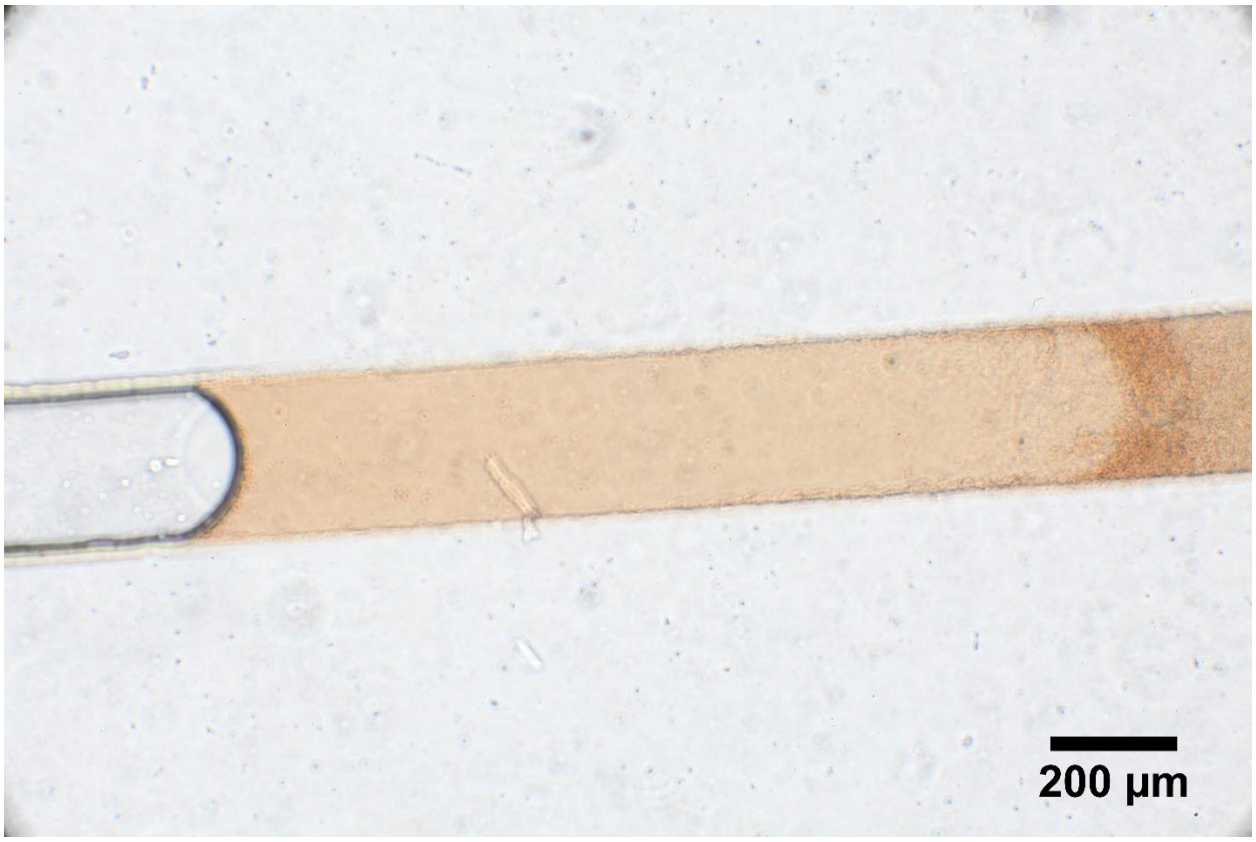

Figure 3: *T-junction is to the left; width of channel is 250um. In the second run, when the chamber was primed with blood, some of it receded and left a gas bubble in the center of the device around the T-junction. Some kind of movement and agglomeration occurred here, although the nature of it is unknown.*

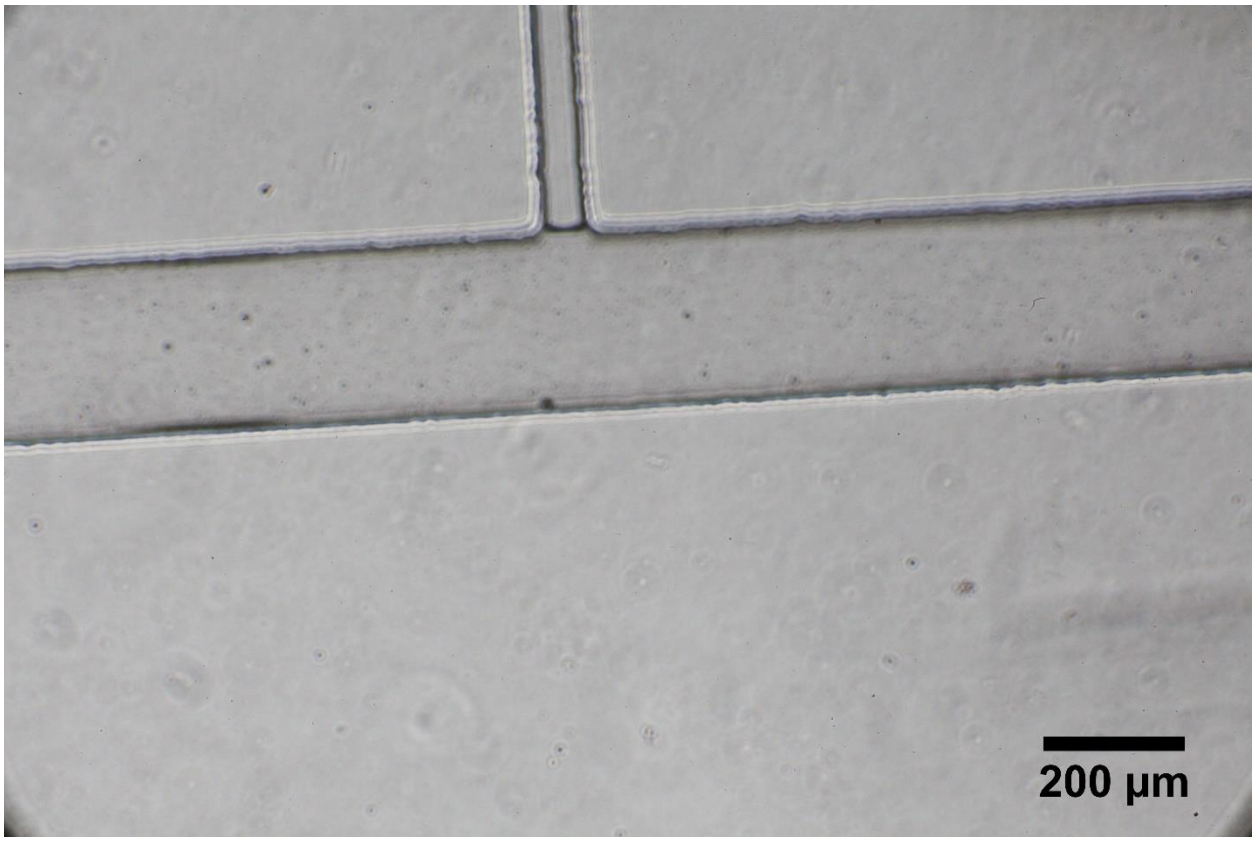

Figure 4: *Run 3 with $CaCl_2$ in the main channel. This fluid later evaporated over the course of the experiment*

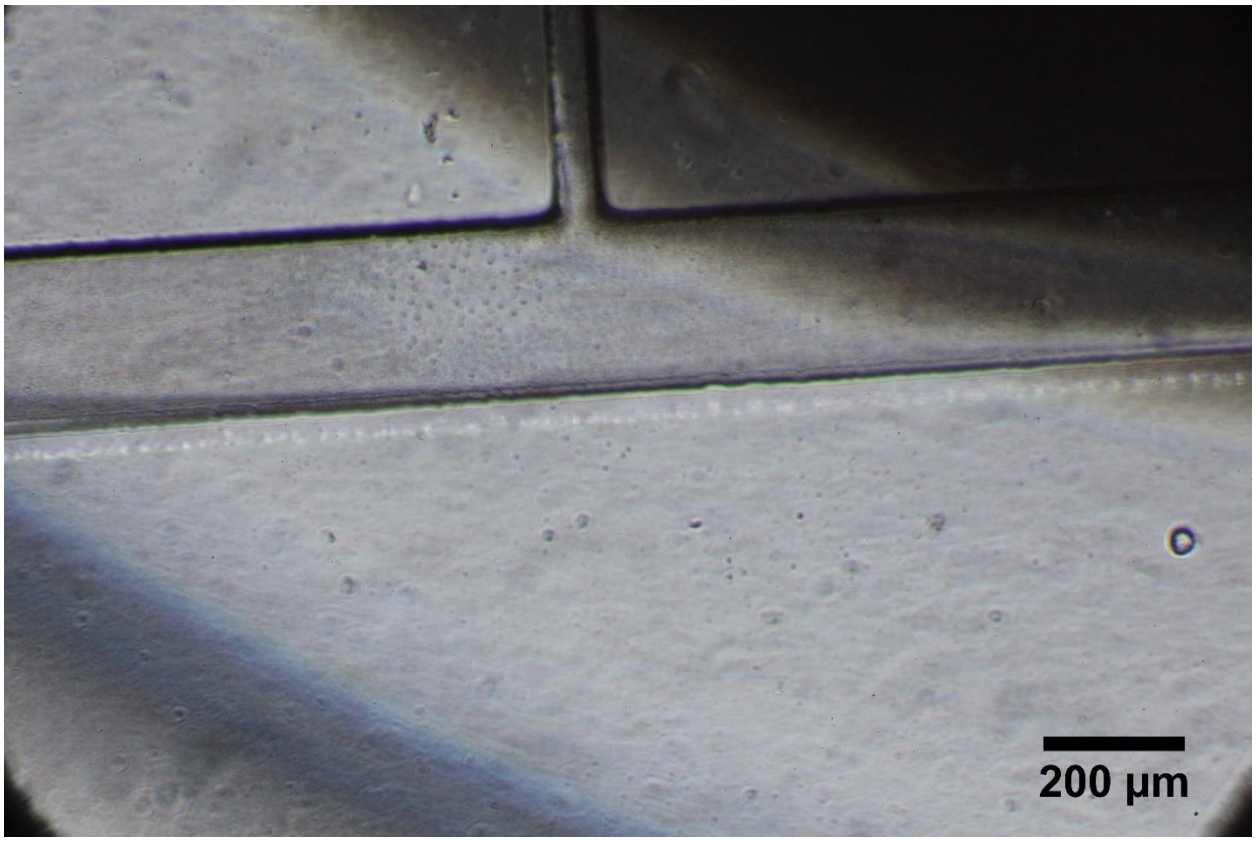

Figure 5**:** *Run 4 was not primed with CaCl2, and blood was able to enter the channel for about 5mm*

Chapter 5 Discussions

5.1 Alternate Plans

Hydrostatic vials do not work well for attempting to get blood flowing in a channel this size. A wider channel could decrease the resistance and therefore the pressure drop needed to let the fluid flow. Another possible solution could be to use a syringe pump at 10uL/min, the intended speed of fluid in the chamber based off a pressure drop of about 50 Pa. Since the device's main chamber holds less than a microliter, this speed ought to have been fast enough to get blood cells visibly moving in the channel. Speeds of up to 60uL/min should be tested in the future with a syringe pump hooked up to the inputs of the device. The syringe can be hooked up to the outlet to pull from both inlets simultaneously.

Blood in this study was treated with EDTA as an anticoagulant. The ferric chloride paper used

sodium citrated blood and recalcified it with $CaCl_2$. EDTA also takes up the calcium and other metal ions in the blood that are critical for the coagulation cascade. Calcium chloride returns the calcium ions to the blood so that clotting is possible again. Although calcium chloride is expected to be used with citrated blood, it may still be able to enable clotting in EDTA-treated blood, too.

5.2 Future Directions

This project was pursued with the hope of generating blood clots to be passed on to our lab's vasculature on a chip device. As tubing would be most ideal for connecting the blood clotting and vasculature devices, having a syringe pump setting the flow rate would be a better option than using hydrostatic vials. The device ought to be kept at 37C along with the tissue culture device growing vasculature on a chip. If exercise on a chip can be developed in our lab, then this clotting device can be coupled with it to model deep vein thrombosis. The embolism is produced in the clotting device, and then passes through the channel and tubing until it reaches the tissue culture device. The thrombus then may stick within the vessels of the tissue culture device, blocking blood flow to part of the chamber. The exercise on a chip device is planned to have oxygen control and pulsatile flow to model oxygen depletion and blood pressure changes from the heart's pulse.

My advisor informed me that molds in the lab usually have as many variations as possible on a single mask. A future mask would include the shorter design with closer inputs for syringe pump use. Although pulling at the outlets is likely to be a more effective method to pull from the two inlets. So hydrostatic vials will sit at the inputs for the blood and ferric chloride, while the output has a syringe pump connected to pull at 10uL/min.

References

1- Di Niso, M., van Es, N., Büller, H. R. (2016) Deep vein thrombosis and pulmonary embolism. *The Lancet, 388*(10063), 3060-3073. doi: 10.1016/S0140-6736(16)30514-1

2- Wudicks, E.F.M. & Scott, J. P. (1997) Pulmonary embolism associated with acute stroke. *Mayo Clinic Proceedings, 72*(4), 297-300. doi: 10.4065/72.4.297

3- Colace, T.V., Muthard, R.W., Diamond, S.L. (2012) Thrombus growth and embolism on tissue factor-bearing collagen surfaces under flow: role of thrombin with and without fibrin. *Arterioscler Tromb Vasc Biol, 32*(6), 1466-1476. doi: 10.1161/ATVBAHA

4- Cardiogenic Brain Embolism: The Second Report of the Cerebral Embolism Task Force. (1989) *Arch Neurol, 46*(7), 727–743. doi:10.1001/archneur.1989.00520430021013

5- Becattini, C. et al. (2005) A prospective study on cardiovascular events after acute pulmonary embolism. *European Heart Journal, 26*(1), 77-83. doi: 10.1093/eurheartj/ehi018

6- Li, M., Hotaling, N.A., Ku D.N., Forest, C.R. (2014) Microfluidic thrombosis under multiple shear rates and antiplatelet therapy doses. *PLoS ONE, 9*(1), e82493. doi: 10.1371/journal.pone.0082493

7- Tsai, M., Kita, A., Leach J., Rounsevell, R., Huang, J.N., Moake, J., Ware, R.E., Fletcher, D.A., Lam, W.A. (2011) In vitro modeling of the microvascular occlusion and thrombosis that occur in hematologic diseases using microfluidic technology. *J Clin Invest, 122*(1), p408-418. doi: 10.1172/JCI58753

8- Colace, T.V., Tormoen, G.W., McCarty, O.J.T, Diamond, S.L. (2013) Microfluidics and coagulation biology. *Annual Review of Biomedical Engineering, 15*, p283-303. doi: 10.1146/annurev-bioeng-071812-152406

9- Welsh, J.D., Colace, T.V., Muthard, R.W., Stalker, T.J., Brass, L.F., Diamond, S.L. (2014) Platelet-targeting sensor reveals thrombin gradients within blood clots forming in microfluidic assays and in mouse. *J Thromb Haemost, 10*(11), p2344-2353. doi: 10.1111/j.1538-7836.2012.04928.x

10- Muthard, R.W., Diamond, S.L. (2013) Side view thrombosis microfluidic device with controllable wall shear rate and transthrombus pressure gradient. *Lab on a Chip, 13*(10), p.1883-1891. doi: 10.1039/C3LC41332B

11- Kurz, K.D., Main, B.W., Sandusky, G.E. (1990) Rat model of arterial thrombosis induced by ferric chloride. *Thromb Res, 60*(4), p269-280

12- Farrehi, P.M., Ozaki, C.K., Cameliet, P., Fay, W.P. (1998) Regulation of arterial thrombosis by plasminogen activator inhibitor-1 in mice. *Circulation, 97*(10), p1002-1008.

13- Wang, X., Smith, P.L., Hsu, M.Y., et al. (2006) Effects of factor XI deficiency on ferric chloride-induced vena cava thrombosis in mice. *J Thromb Haemost, 4*(9), p1982-1988.

14- Eckly, A., Hechler, B., Freund, M., et al. (2011) Mechanisms underlying $FeCl_3$-induced arterial thrombosis. *J Thromb Haemost, 9*(4), p779-789.

15- Barr, J.D., Chauhon, A.K, Schaeffer, G.V., Hansen, J.K., Motto, D.G. (2013) Red blood cells mediate the onset of thrombosis in the ferric chloride murine model. *Blood, 121*(18), p3633-3741.

16- Ciciliano, J.C., Sakurai, Y., Myers, D.R. et al. (2015) Resolving the multifaceted mechanisms of the ferric chloride thrombosis model using an interdisciplinary microfluidic approach. *Blood, 126*(6), p817-824.

17- Pandian, N.K.R., Mannino, R.G., Lam, W.A., Jain, A. (2018) Thrombosis-on-a-chip: Prospective impact of microphysiological models of vascular thrombosis. *Current Opinion in Biomedical Engineering*, *5*, p29-34.

18- Jagadeeswaran, P., Cooley, B.C., Gross, P.L., Mackman, N. (2016) Animal models of thrombosis from zebrafish to nonhuman primates: Use in the elucidation of new pathologic pathways and the development of antithrombotic drugs. *Circulation Research*, *118*(9), p1363-1379.

19- Zhang, C., Neelamegham, S. (2017) Application of microfluidic devices in studies of thrombosis and hemostasis. *Platelets, 28*(5), p434-440.

20- Herbig, B. A., Yu, X., & Diamond, S. L. (2018). Using microfluidic devices to study thrombosis in pathological blood flows. *Biomicrofluidics, 12*(4), 042201.

21- Sobrino, A., Phan, D.T.T, Datta, R., Wang, X., Hachey, S.J., Romero-Lopez, M., Gratton, E., Lee, A.P., George, S.C., Hughes, C.C.W. (2016) 3D microtumors in vitro supported by perfused vascular networks. *Scientific Reports, 6*(31589). DOI: 10.1038/srep31589.

22- Grosse, S.D., Nelson, R.E., Nyarko, K.A., Richardson, L.C., Raskob, G.E. (2016) The economic burden of incident venous thromboembolism in the United States: a review of estimated attributable healthcare costs. *Thromb Res*, *137,* p3-10.